Chapter 1

Tunable High-Power External-Cavity GaN Diode Laser Systems in the Visible Spectral Range

Mingjun Chi, Ole Bjarlin Jensen,
Anders Kragh Hansen and Paul Michael Petersen

Additional information is available at the end of the chapter

http://dx.doi.org/10.5772/intechopen.79703

Abstract

In this chapter, both blue and green high-power tunable diode laser systems based on GaN broad-area diode laser (BAL) in Littrow external cavity are demonstrated. For blue diode laser system, for high-power application, an output power around 530 mW over a 1.4 nm tunable range is obtained; for wide tunable range application, an output power around 80 mW over a 6.0 nm tunable range is obtained. For the green diode laser system, for high-power application, an output power around 480 mW with a tunable range of 2.1 nm is achieved; for wide tunable range application, an output power of 50 mW with a tunable range of 9.2 nm is achieved. The tuning range and output power optimization of an external-cavity diode laser system is investigated based on the experimental results obtained in the blue and green external-cavity GaN diode laser systems. The obtained results can be used as a guide for selecting gratings for external-cavity diode lasers for different requirements. The temporal dynamics of the green diode laser system is studied experimentally, and pulse package oscillation is observed, for the first time to our knowledge, in a BAL with an external-cavity grating feedback.

Keywords: diode lasers, GaN, external cavity, tunable, instabilities and chaos

1. Introduction

Since the first demonstration of a room temperature continuous wave (CW) GaN violet diode laser by Nakamura et al. [1], great progress has been achieved on the GaN-based diode lasers in the violet to green spectral range. Nowadays, high-power GaN diode lasers with CW output power of a few watts are commercially available in the blue to green spectral range [2].

The spectral bandwidth of the high-power devices is around 1.0 nm, and the devices are not tunable. Although single longitudinal mode GaN diode laser around 405 nm has been achieved with the laterally coupled distributed feedback (DFB) technique [3]; this technique is under development and not available for commercial devices, especially not available for high-power GaN diode lasers.

Tunable, high-power, narrow spectral bandwidth light sources based on semiconductor lasers from the violet to green spectral range are attractive for many applications, such as high-resolution spectroscopy, holographic data storage, laser cooling, laser holographic display, biophotonics and as pump sources for nonlinear frequency conversion and for titanium-sapphire lasers [4–10]. The broad emission bandwidth limits the usage of the high-power GaN diode lasers in some of these applications. There are two main techniques to achieve high-power, narrow-bandwidth blue and green laser emission based on semiconductor devices. The first one is based on nonlinear frequency conversion, including second harmonic generation and sum frequency generation of GaAs lasers emitting from 800 to 1100 nm [11, 12]. The second approach is external-cavity feedback technique used to improve the spectral quality of the high-power GaN diode lasers and make the lasers tunable [13, 14]. The laser systems developed based on the first method are relatively complex, and the laser systems are not tunable, or the tunable range is narrow. Thus, the second approach is applied in this chapter to achieve narrow bandwidth, tunable blue and green diode laser systems.

In this chapter, we first demonstrate two tunable, narrow bandwidth high-power GaN diode laser systems; one system is emitting around 455 nm in the blue spectral region, the other is emitting around 515 nm in the green spectral region. Secondly, the tuning range and output power optimization of an external-cavity diode laser (ECDL) system is investigated based on the experimental results. Finally, the dynamics of the green external-cavity diode laser system is studied.

2. Experimental setup

The experimental setup for the Littrow external-cavity feedback system is schematically shown in **Figure 1**. The high-power GaN diode lasers (2 W for blue or 1 W for green devices) used in our experiment are broad-area diode lasers. The laser beam is TE-polarized for both devices. The laser beam emitted from the front facet is collimated by an aspherical lens of 4.0 mm focal length with a numerical aperture of 0.6. The collimated beam is incident on a bulk diffraction grating mounted in Littrow configuration and oriented with the lines in the grating parallel to the slow axis of the diode laser.

The first-order diffracted beam from the grating is the feedback beam, thus the external cavity is formed between the diode laser and the grating. A beam splitter is inserted in the external cavity and reflects part of the beam as a diagnostic beam in which the spectral bandwidth and tunability of the laser system are measured. The zeroth-order diffracted beam of the grating is the output beam of the ECDL system, and a power meter is used to record the power of the output beam. The ECDL system is tuned by rotating the grating along the groove direction.

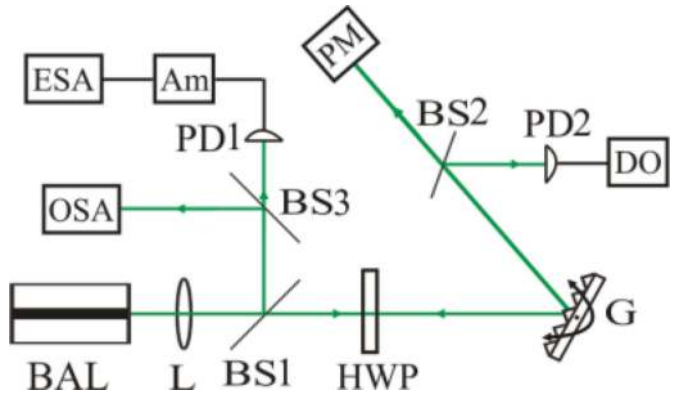

Figure 1. Experimental setup of the ECDL system. BAL, broad-area diode laser; L, lens; BS1, BS2 and BS3, beam splitter; HWP, half-wave plate; G, bulk grating, PD1 and PD2, photodiode; DO, digital oscilloscope; OSA, optical spectrum analyzer; Am, amplifier; ESA, electrical spectrum analyzer; PM, power meter.

3. Experimental results

3.1. Blue GaN external-cavity diode laser system

In this subsection, the results of blue ECDL system are presented [15]. Two bulk diffraction gratings are used in the blue ECDL system, one is a holographic diffraction grating with a groove density of 2400 lines/mm (Thorlabs, GH13-24 U), and the zeroth- and first-order diffraction efficiencies are 78.8 and 8.3%. The other is a ruled diffraction grating that is ruled with 1800 lines/mm and has a blaze wavelength of 500 nm (Thorlabs, GR13-1850), the zeroth- and first-order diffraction efficiencies are 29.6 and 53.5%, respectively. The length of the external cavity is around 110 mm.

In the freely running condition, the threshold current of the laser device is around 0.12 A, and the slope efficiency is around 1.62 W/A. With an injected current of 1.4 A, a 2 W output power is obtained. The diode laser is operating in multiple Fabry-Perot (FP) modes. The spectrum is centered around 456 nm with a spectral bandwidth around 1.2 nm. The longitudinal mode spacing of the FP modes is around 28.5 pm.

The blue ECDL system is characterized by measuring the spectrum at different wavelengths with these two different gratings. **Figure 2** shows the spectra of the blue ECDL system with an output power around 85 mW for both gratings. For the ECDL system with the holographic diffraction grating at an injected current of 0.2 A, **Figure 2(a)** shows seven normalized spectra from 453.4 to 456.5 nm. The bandwidth of the spectrum (FWHM) is around 9 pm in the 3.1 nm tunable range; it is much less than the 28.5 pm mode space of the FP laser resonator; this means the laser is forced to operate in a single longitudinal FP mode by the external feedback. **Figure 2(b)** shows eight normalized spectra from 452.8 to 458.8 nm for the ECDL system with the ruled diffraction grating at an injected current of 0.3 A. The spectral bandwidth is less than 20 pm for wavelengths longer than 456 nm in the 6.0 nm tunable range; for shorter wavelengths, the spectral bandwidth is less than 42 pm, that is, two FP modes oscillate simultaneously. The amplified spontaneous emission (ASE) is more than 20 dB suppressed in the tunable ranges for both diffraction gratings.

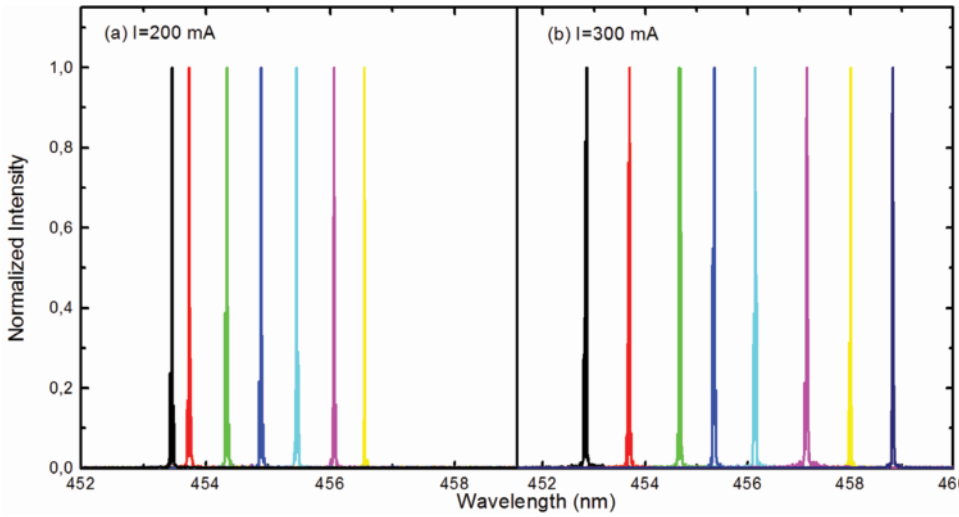

Figure 2. Optical spectra of the output beam from the blue ECDL system with (a) a holographic grating and (b) a ruled grating. The output power is around 85 mW.

Figure 3 shows the spectra of the blue ECDL system with an output power around 200 mW with both gratings. **Figure 3(a)** shows seven normalized spectra from 453.7 to 456.5 nm with the holographic grating, at an injected current of 0.3 A. The spectral bandwidth is around 35 pm in the tunable range, that is, two FP modes oscillate simultaneously. **Figure 3(b)** shows the normalized spectra of the ECDL from 453.5 to 459.0 nm with the ruled grating, the injected current is 0.6 A. The bandwidth is less than 67 pm in the tunable range. The ASE suppression is more than 24 dB for the holographic grating feedback and more than 17 dB for the ruled grating feedback.

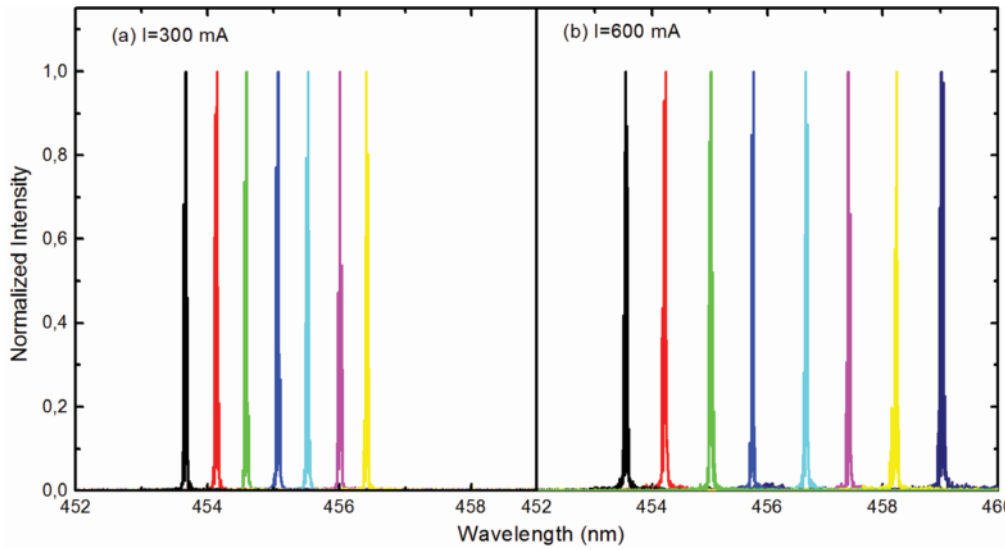

Figure 3. Optical spectra of the output beam from the blue ECDL system with (a) a holographic grating and (b) a ruled grating. The output power is around 200 mW.

Figure 4 shows the spectra of the blue ECDL system with an output power around 350 mW. The laser system is tunable from 454.1 to 456.5 nm for the holographic grating feedback. The bandwidth is around 35 pm in the tunable range, and the ASE is more than 24 dB suppressed. The laser system is tunable from 455.3 to 459.4 nm for the ruled grating feedback; the ASE is more than 18 dB suppressed. The bandwidth (FWHM) is less than 70 pm in the tunable range, but side peaks appear in some spectra as shown in **Figure 4(b)**.

With the ruled grating, a further increase of the current increases the spectral bandwidth to a few hundred picometers, and two peaks are present in the spectrum. With the holographic grating, the current can be increased to 0.6 A, where the diode laser is tuned from 455.0 to 456.4 nm with an output power of around 530 mW. The bandwidth is around 63 pm in the tunable range, and the ASE is more than 20 dB suppressed. Further increase of the current also increases the bandwidth to a few hundred picometers for the ECDL with the holographic grating.

The output power of the blue ECDL system at different wavelengths is shown in **Figure 5** with these two different gratings. When the holographic grating is applied, the maximum output powers are 85, 198, 368 and 531 mW with injected current of 0.2, 0.3, 0.45 and 0.6 A, respectively. When the ruled grating is applied, the maximum output powers are 90, 222, and 340 mW with injected current of 0.3, 0.6 and 0.9 A, respectively. For both gratings, the output power is relatively constant in the tunable range at each injected current. With the highest output power of the ECDL, that is, 531 mW for the holographic grating feedback and 340 mW for the ruled grating feedback, around 68 and 27% of the output power of the freely running laser are extracted in the ECDL system for the two gratings, respectively. Thus, the efficiency of the ECDL with the holographic grating is much higher than that of the ECDL with the ruled grating. The reason is the higher first-order diffraction efficiency of the ruled grating (53.5%) limits the output power.

The tunable range of the blue ECDL system with the ruled grating is much broader than that of the blue ECDL system with the holographic grating when the output power of the diode

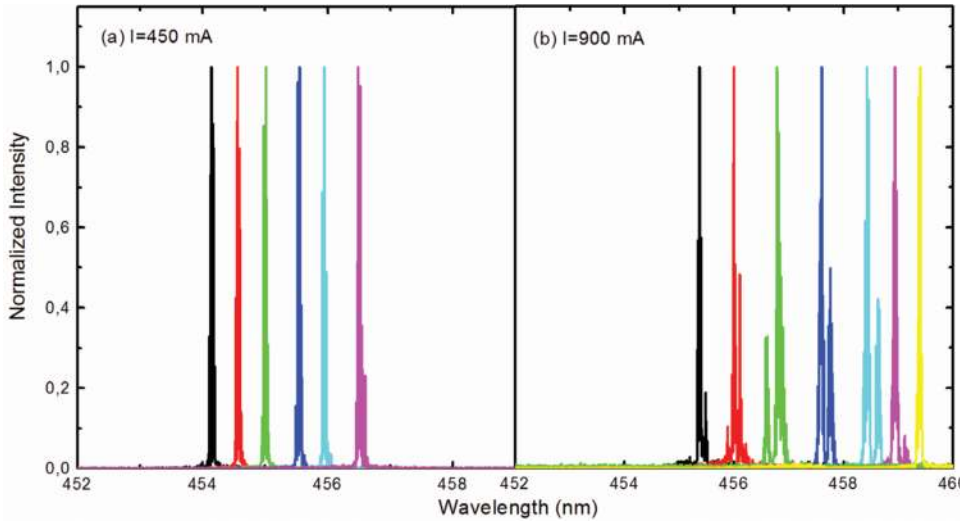

Figure 4. Optical spectra of the output beam from the ECDL system with (a) a holographic grating at an injected current of 0.45 A and (b) a ruled grating at an injected current of 0.9 A.

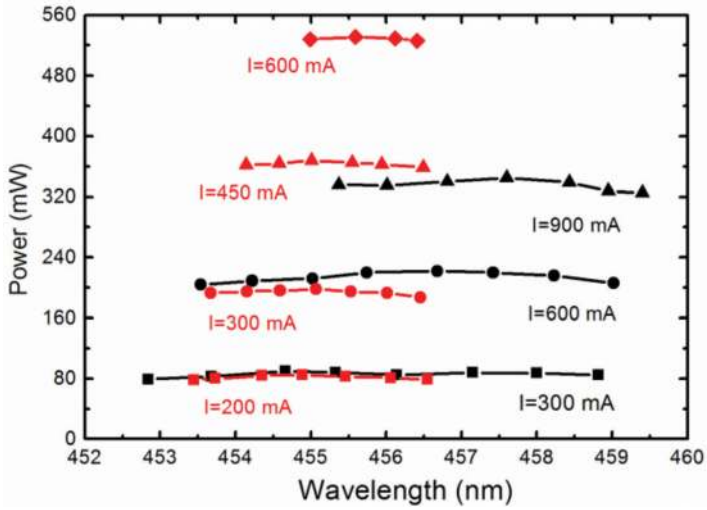

Figure 5. Output power of the blue ECDL at different wavelengths and operating currents with the holographic grating (red signs) and the ruled grating (black signs).

laser system is comparable. The reason is that the first-order diffraction efficiency of the ruled grating is much higher compared with that of the holographic grating, that is, 53.5 versus 8.3%. The higher the feedback strength from the grating, the more effective the suppression of the freely running lasing modes.

In summary, a high-power, tunable, narrow-bandwidth ECDL system based on a GaN diode laser around 455 nm is demonstrated. The laser system can be tuned over 1.4 nm with an output power around 530 mW when the holographic grating is applied; the laser system can be tuned over 6.0 nm with an output power of 80 mW when the ruled grating is applied. The results show the efficiency of the ECDL with holographic grating is higher, but the tunable range of the ECDL with ruled grating is broader.

3.2. Green GaN external-cavity diode laser system

In this subsection, the results of a green ECDL system are presented [16]. For the green ECDL system, only the holographic grating (Thorlabs, GH13-24 U) is applied. A half-wave plate is inserted in the external cavity to turn the polarization direction of the laser beam. Thus, the green laser system can be operated in both *s*-polarized mode (the laser beam is polarized along the lines of the grating) and *p*-polarized mode (the laser beam is polarized perpendicular to the lines of the grating). The zeroth- and first-order diffraction efficiencies of the grating are around 81 and 7% for the *s*-polarized beam, and around 48 and 29% for the *p*-polarized beam, respectively. The length of the external cavity of the laser system is around 140 mm, corresponding to a 0.95 pm external-cavity mode spacing.

The threshold current of the freely running green diode laser is around 0.25 A, and the slope efficiency is around 1.0 W/A. With an injected current of 1.4 A, 1.1 W output power is obtained. The laser diode is operating in multiple FP modes centered around 515 nm, with a spectral bandwidth of 1.3 nm. The mode spacing of the FP modes is around 39 pm.

The tunability of the green ECDL system operated in both *s*- and *p*-polarized modes is characterized by measuring the optical spectrum of the output beam at different wavelengths. The spectra of the ECDL for both operating modes with an operating current of 330 mA are shown in **Figure 6**. The output power of the green ECDL system for the *s*-polarized and *p*-polarized mode operation are around 70 and 50 mW, respectively. **Figure 6(a)** shows eight normalized spectra from 511.1 to 516.0 nm for *s*-polarized mode operation. The spectral bandwidths of these spectra are around 8 pm. Compared with the 39 pm mode spacing of the FP modes, the ECDL in the *s*-polarized mode operates in single FP mode. **Figure 6(b)** shows 10 spectra from 508.8 to 518 nm for *p*-polarized mode operation. The bandwidth is less than 9 pm in the tunable range. The ASE is more than 15 and 17 dB suppressed for *s*- and *p*-polarized mode operation, respectively.

Figure 7 shows the optical spectra of the green ECDL system for both operation modes with the output power around 290 mW. To achieve the 290 mW output power, 600 and 850 mA injected currents are needed for *s*- and *p*-polarized mode operation, respectively. Six normalized spectra from 513.1 to 515.7 nm are shown in **Figure 7(a)** for *s*-polarized mode operation. Two peaks are observed in the spectra and the spectral bandwidth is less than 0.25 nm. Five spectra from 512.9 to 517.5 nm are shown in **Figure 7(b)** for *p*-polarized mode operation. The spectral bandwidth (FWHM) is less than 50 pm in the tunable range, however side modes appear in the spectra. The ASE is more than 15 dB suppressed in the tunable ranges for both *s*- and *p*-polarized mode operation. In the *s*-polarized mode, the injected current can be further increased to 850 mA, and the output power is increased to 480 mW. The ECDL system can be tuned from 514.1 to 516.2 nm, the emission bandwidth is less than 0.5 nm in the tunable range, and the ASE is more than 15 dB suppressed.

Figure 8 shows the output power of the ECDL system at different wavelengths and injected currents for both operating modes. In the *s*-polarized mode, the maximum output powers

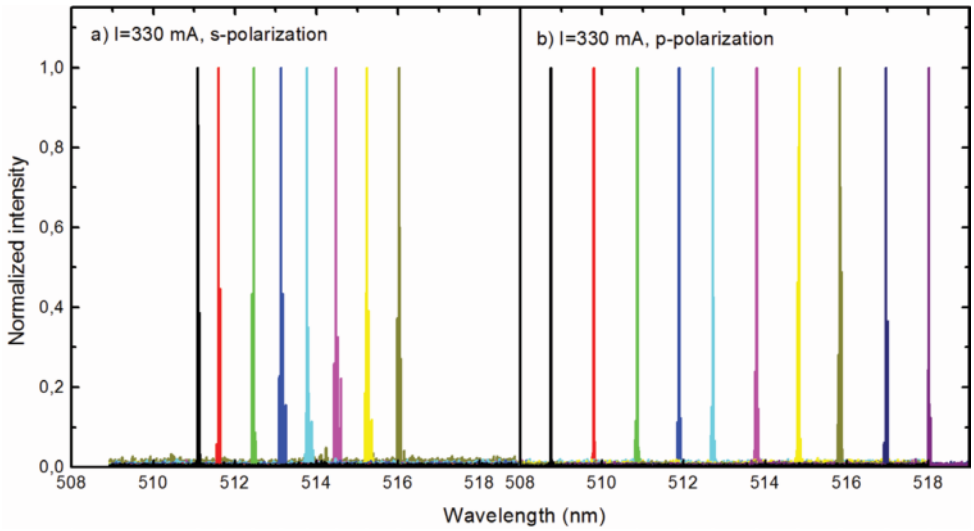

Figure 6. Optical spectra of green ECDL system operates in (a) *s*-polarized mode and (b) *p*-polarized mode. The injected current is 330 mA for both conditions.

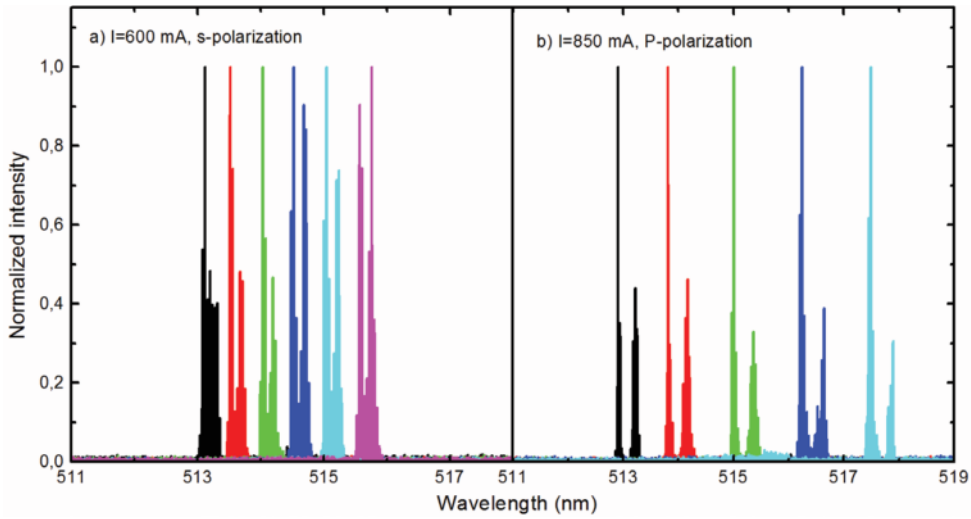

Figure 7. Optical spectra of the green ECDL system operates in (a) *s*-polarized mode and (b) *p*-polarized mode. The output power is around 290 mW for both operation modes.

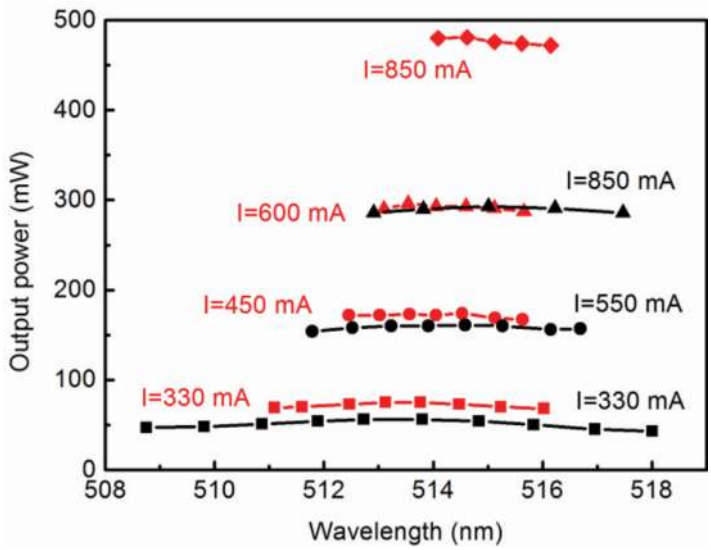

Figure 8. Output power of the ECDL at different wavelengths and operating currents, operated in *s*-polarized mode (red signs) and *p*-polarized mode (black signs).

of the ECDL are 75, 173, 296 and 481 mW with injected current of 330, 450, 600 and 850 mA, respectively. In the *p*-polarized mode, the maximum output powers are 56, 161 and 293 mW with injected current of 330, 550 and 850 mA, respectively. The output power is relatively constant in the tunable range at each injected current for both operating modes.

With the highest injected current, that is, 850 mA, the maximum output powers for the *s*- and *p*-polarized mode operation are 481 and 293 mW. This means that 75 and 46% of the output power in freely running condition is extracted in the ECDL system for the *s*- and *p*-polarized

mode operation. However, **Figure 8** shows the tunable range of the ECDL in *p*-polarized mode operation is much broader than that of the ECDL in the *s*-polarized mode operation. The main reason for this difference is the higher zeroth-order diffractive efficiency of the holographic grating for the *s*-polarized beam compared with that for the *p*-polarized beam, that is, 81 versus 48%. The higher zeroth-order diffraction efficiency of the grating for *s*-polarized beam means a high output coupling efficiency, that is, high output power. However, the first-order diffractive efficiency for the *p*-polarized beam is much higher than that for the *s*-polarized beam, that is, 29 versus 7%. The higher the feedback strength from the grating (the higher first-order diffraction efficiency), the more effective the suppression of the freely running lasing mode, thus the tunable range of the green ECDL system operated in the *p*-polarized mode is broader.

In summary, a high-power, tunable, narrow-bandwidth ECDL system based on a GaN device around 515 nm is demonstrated. The laser system can be tuned over 2.1 nm with an output power around 480 mW in the *s*-polarized mode operation; the laser system can be tuned over 9.0 nm with an output power of 50 mW in the *p*-polarized mode operation. We can choose different operating modes for different priorities, that is, high-power or broad tuning range, using only one ECDL system.

3.3. Selection of diffraction grating for ECDL

Both the blue and green tunable ECDL systems show the efficiency (output power) of the ECDL system is higher when the zeroth-order diffraction efficiency of the grating used in the laser system is higher, such as the conditions for the holographic grating in the blue diode laser system and the *s*-polarized mode operation for the green diode laser system. However, the tunable range of the ECDL system with higher efficiency is narrower since a higher first-order diffraction efficiency of the grating is needed to achieve a wider tunable range. Thus, there is a compromise between the output power and the tunable range of the ECDL system since the sum of the zeroth- and first-order diffraction efficiencies is around unity.

To understand this compromise between the efficiency (output power) and tunable range further, a theoretical analysis is given below based on rate equations of the diode laser. The rate equations describing the carrier density N and the photon density N_{ph} in the diode laser cavity are given as [15, 17]:

$$\frac{dN}{dt} = \frac{\eta_i j}{qd} - \frac{N}{\tau} - v_{gr} g(N) N_{ph}, \tag{1}$$

$$\frac{dN_{ph}}{dt} = v_{gr} \Gamma g(N) N_{ph} - \frac{N_{ph}}{\tau_{ph}} + \alpha_m v_{gr} K N_{ph}(t - t_0), \tag{2}$$

where j is the inject current density, η_i is the internal efficiency, q is the elementary charge of an electron, d is the thickness of the active region, τ is the carrier lifetime, v_{gr} is the group velocity of the photons, $g(N)$ is the material gain, Γ is the confinement factor, τ_{ph} is the photon lifetime, α_m is the mirror loss, K is the feedback strength of the grating (the first-order diffraction efficiency in our case, here the other loss in the cavity is neglected.), t_0 is the time delay of

the external cavity. In particular $1/\tau_{ph} = v_{gr}(\alpha_i + \alpha_m)$, where α_i is the internal loss; and the gain $g(N) = g_N(N-N_{tr})$, g_N is the differential gain coefficient and N_{tr} is the transparency carrier density. When the diode laser system is steady-state operated, rearrange Eqs. (1) and (2), we obtain:

$$dN/dt = \eta_i j/qd - N/\tau - v_{gr} g_N(N - N_{tr}) N_{ph}, \tag{3}$$

$$dN_{ph}/dt = v_{gr} \Gamma g_N(N - N_{tr}) N_{ph} - v_{gr}[\alpha_i + (1 - K)\alpha_m] N_{ph}. \tag{4}$$

Eq. (4) shows the effect of the feedback is to reduce the mirror loss from α_m to $(1-K)\alpha_m$.

The steady-state solution of Eqs. (3) and (4) can be obtained as:

$$N = N_{tr} + \frac{1}{\Gamma g_N \tau_{ph} v_{gr}} - \frac{K\alpha_m}{\Gamma g_N} = N_{th}(0) - \frac{K\alpha_m}{\Gamma g_N}, \tag{5}$$

$$N_{ph} = \frac{\eta_i \Gamma \tau_{ph}}{qd}[j - j_{th}(K)] \frac{1}{1 - K\alpha_m/(\alpha_i + \alpha_m)}, \tag{6}$$

$$j_{th}(K) = j_{th}(0) - qdK\alpha_m/\eta_i \tau\Gamma g_N, \tag{7}$$

where $N_{th}(0)$ is the threshold carrier density without feedback, and $j_{th}(0) = qdN_{th}(0)/\eta_i\tau$ is the threshold current density without feedback. Eq. (7) shows the threshold current density $j_{th}(K)$ is decreased with the feedback strength K. Eq. (6) shows the photon density increases with K.

In our experiment, when we rotate the grating further to operate the laser system outside of the tunable ranges, the freely running emission appears and dominates the laser output, this means the competition of the freely running lasing at the gain center λ_0 and the lasing at wavelength λ (with a distance from the gain center) with feedback determines the tunable range of the external-cavity diode laser system. **Figure 9** shows a schematic diagram of the gain and the threshold of the diode laser system; the grating feedback profile is also shown. The grating feedback decreases the threshold current density at λ from $j_{th}(\lambda, 0)$ to $j_{th}(\lambda, K)$. When $j_{th}(\lambda, K)$ is less than the freely running threshold current density at λ_0, that is, $j_{th}(\lambda_0, 0)$, the laser system lases at λ, and vice versa. Since the decrease of the threshold current density by the feedback is proportional to K, a higher value of K causes a wider tunable range of the external-cavity diode laser system.

The output power P of an external-cavity diode laser system can be expressed as:

$$P \propto N_{ph}(1 - K) = \frac{\eta_i \Gamma \tau_{ph}}{qd}[j - j_{th}(K)] \frac{1 - K}{1 - K\alpha_m/(\alpha_i + \alpha_m)}. \tag{8}$$

The slope efficiency of the laser system decreases with the feedback strength K due to the last term in Eq. (8). Thus, the output power decreases with K, when the laser system is operated far above the threshold; although the threshold of the laser system also decreases with the feedback strength K.

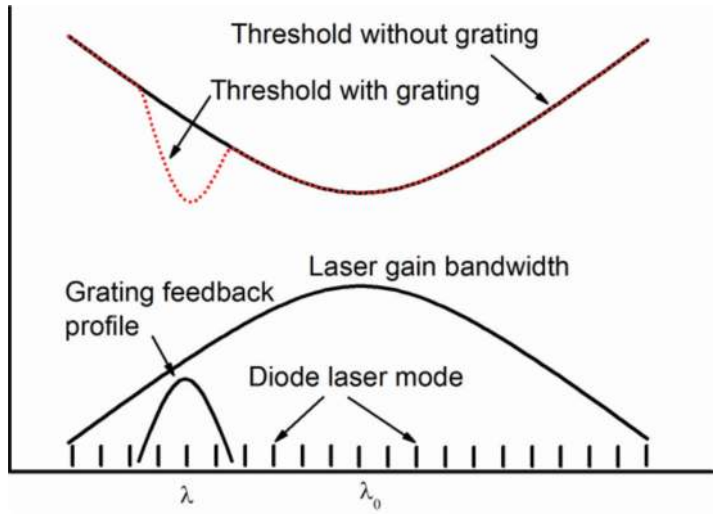

Figure 9. Schematic diagram of the gain and threshold with and without grating feedback. The grating feedback profile is also shown.

The theoretical analysis above mentioned is in agreement with our experimental results obtained from the blue and green ECDL systems; where the green laser system in *p*-polarized mode (high first-order diffraction efficiency) has a much wider tunable range but less output power compared with the laser system in *s*-polarized mode (low first-order diffraction efficiency). The experimental results in Refs. [18, 19] also show that wider tunable ranges and low output powers of the ECDLs were achieved with gratings with higher first-order diffraction efficiencies. From both the theoretical and experimental results, we can conclude that the compromise between the output power and the tunable range of an ECDL is a general condition and irrelevant to the geometry of the external cavity.

Considering the results obtained from the blue ECDL system using two different diffraction gratings, the ECDL system with the holographic grating has a narrower spectral bandwidth and a larger suppression of ASE when the output power of the ECDL with the two gratings are comparable. We believe the reason is that the holographic grating has a larger groove density compared with ruled grating, that is, 2400 lines/mm for the holographic grating versus 1800 lines/mm for the ruled grating, meaning that the holographic grating has a higher spectral resolution.

Both the experimental results and the theoretical analysis here provide a general guide to the selection of gratings for ECDL systems. Two main parameters of a diffraction grating are considered when a grating is used to build an ECDL system: the groove density and the first-order diffraction efficiency. A grating with a larger groove density leads to a narrower spectral bandwidth and a higher suppression of ASE compared with a grating with a small groove density. If a higher output power of a laser system is prioritized, a grating with a lower first-order diffraction efficiency should be selected. If a wider tunable range of a laser system is the high priority, a grating with a higher first-order diffraction efficiency should be selected. Thus, there is a compromise between the output power and the tuning range of an ECDL system. This is the main consideration for selecting a diffraction grating to build an ECDL system.

3.4. Dynamics of the green ECDL system

When external-cavity feedback is applied to a diode laser, complex temporal dynamics may take place [20, 21]. Thus, it is important for us to investigate the dynamics of the developed visible ECDL systems based on the GaN devices. In this subsection, we study the dynamic behaviors of the green ECDL system operated in *p*-polarized mode [22].

The complex dynamic behaviors have been studied intensively for both narrow-stripe diode lasers [23–26] and BALs [27–36] with external feedback. The dynamics of BALs have been investigated with short-cavity feedback [27–29], long-cavity feedback [30–32], tilt mirror feedback [33, 34] and lateral-mode-selected feedback [35, 36]. The feedback elements include ordinary mirrors [29–34], phase-conjugate mirrors [30] and spatially filtered mirrors [27, 28, 35, 36]. Different dynamic behaviors, such as low-frequency fluctuations (LFFs) [30, 31], self-pulsation [35], periodic oscillations [33, 36], pulse package oscillation (PPO) [28, 29, 36] and chaos [32], have been observed in the BALs with different external feedback. External grating feedback is widely used to achieve tunable high-power BAL systems [13–16]. However, the dynamics of such systems have only been studied in a very few cases [37].

As shown in **Figure 1**, the beam splitter, BS1, inserted in the external cavity reflects part of the beam to a silicon PIN photodiode, PD1, after a high-frequency amplifier; the amplified electronic signal is sent to an electrical spectrum analyzer to measure the intensity noise spectrum. The second beam splitter, BS2, reflects part of the output beam to the second photodiode, PD2, and a digital oscilloscope is used to measure the time series of the generated electronic signal. Since the green ECDL system is operated in *p*-polarized mode, the first-order diffraction efficiency is around 29%. Assuming a coupling efficiency of the feedback beam into the laser cavity is 50%, the feedback strength is around 14.5%, a moderate feedback strength for BALs [29, 35]. The physical length of the external cavity is around 33 cm.

The threshold current of the BAL is decreased from 250 to 205.5 mA by the external grating feedback. The wavelength is around 511.9 nm. We keep the feedback grating untouched during the experiment, meaning both the length of the external cavity and the wavelength of the green ECDL system are unchanged.

We investigate the dynamic behaviors of the green ECDL system by increasing the injected current from just above the threshold to more than two times threshold. **Figure 10(a)** shows the time series of the output beam with an operating current of 206.9 mA; a low-frequency periodic oscillation with a period around 220 ns is observed. The inset of **Figure 10(a)** shows the details of the time series in short time scale, an oscillation with a period around 2.4 ns is observed, the period of this oscillation is equal to the external-cavity delay time. This high-frequency oscillation is named as external-cavity oscillation with single-round-trip external-cavity frequency ν_{EC} [28, 35]. **Figure 10(b)** shows the intensity noise spectrum of the output beam. Besides the peak at ν_{EC}, a peak round 4.5 MHz and its harmonics for the low-frequency oscillation (LFO) shown in **Figure 10(a)**, ν_{LFO}, are observed. Additionally, some peaks around ν_{EC} with the frequency difference of ν_{LFO} are also visible. **Figure 10** shows that the output of the green ECDL manifests a typical dynamic state named regular PPO, which mainly takes place in short cavity feedback condition [28, 29], where the external-cavity loop oscillation is modulated by a periodic LFO.

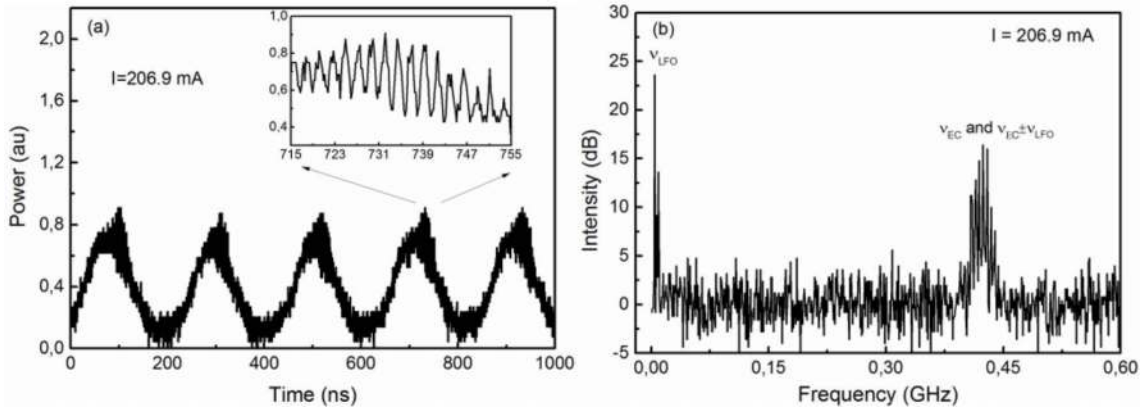

Figure 10. (a) Time series and (b) intensity noise spectrum of the output beam from the green ECDL system with an operating current of 206.9 mA. The inset in (a) shows a close-up of the peak of one of the pulse packages.

Figure 11 shows the time series of the output beam of the green ECDL system with operating currents of 211 and 213 mA. We can observe the periodic LFO for both injected currents. The corresponding oscillation frequencies are around 20 and 29 MHz with 211 and 213 mA injected currents, respectively. For both injected currents, we can observe the pulse packages consisted of pulses occurring at the external-cavity delay interval, this means the regular PPO takes place for both injected currents. The oscillation frequency of the regular PPO, ν_{LFO}, observed in **Figures 10** and **11** show its increase with the current injected to the laser device. This phenomenon was also observed in an integrated semiconductor laser with short-cavity feedback [38]. The intensity noise spectra with these two injected currents are also measured; the results are similar to the results shown in **Figure 10(b)** and consistent with the time series shown in **Figure 11**.

The operating current is increased until to 420 mA, that is, more than twice the threshold of the ECDL system. The measured time series and intensity noise spectra at injected currents of

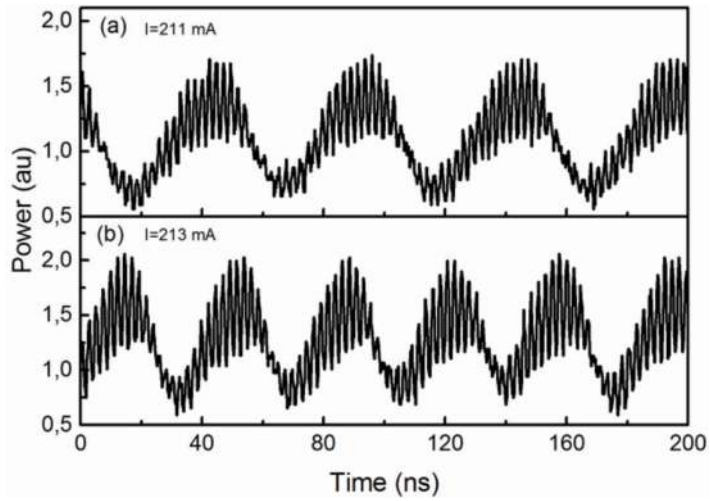

Figure 11. Time series of the output beam from the green ECDL system with an injected current of (a) 211 mA and (b) 213 mA.

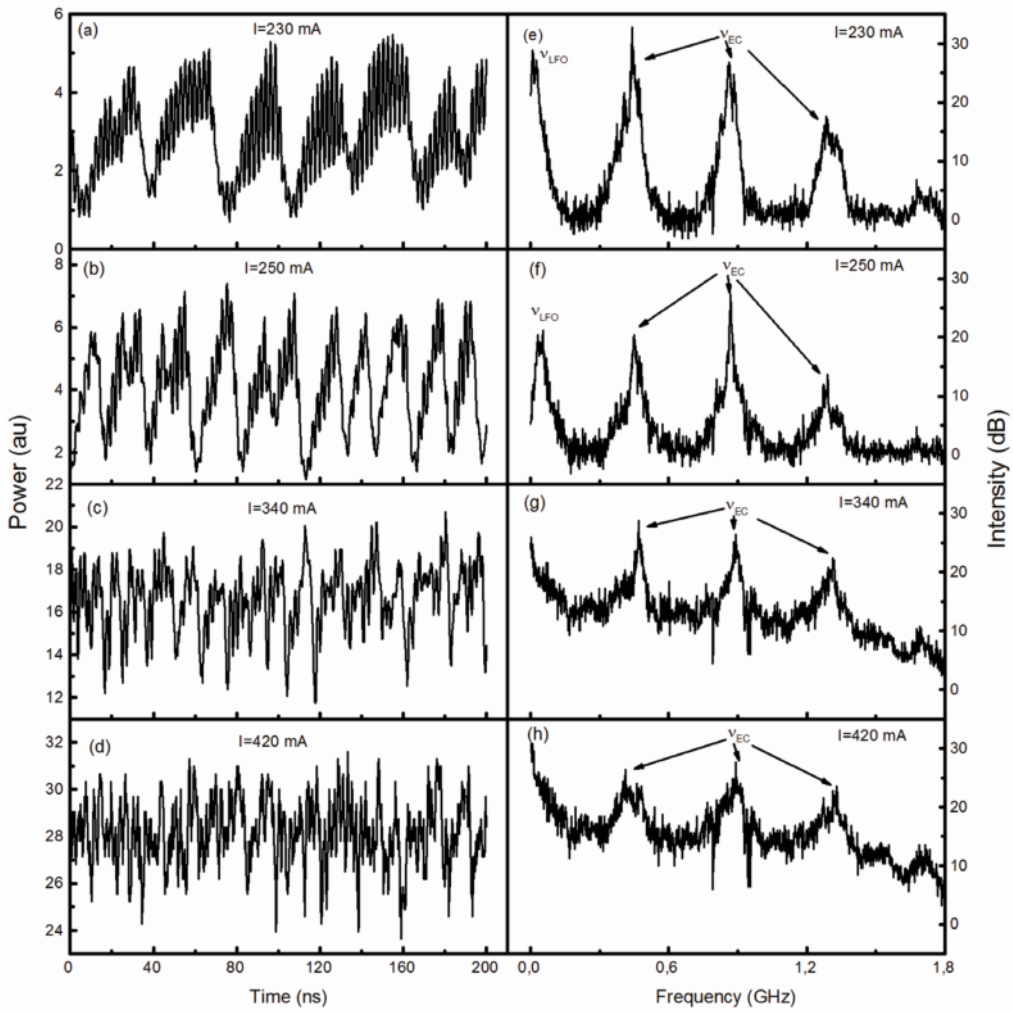

Figure 12. Time series and intensity noise spectra of the output beam from the green ECDL with the injected current of (a, e) 230 mA, (b, f) 250 mA, (c, g) 340 mA and (d, h) 420 mA.

230, 250, 340 and 420 mA are shown in **Figure 12**. The pulse packages first oscillate irregularly, as shown in **Figure 12(a**, **e)** with an injected current of 230 mA. The time series in **Figure 12(a)** shows the pulse packages consisting of the pulse train with the period of external-cavity delay time oscillate irregular. The intensity noise spectrum in **Figure 12(e)** shows the peak for LFO and peaks for external-cavity oscillation at multiples of ν_{EC}. However, the peaks at $\nu_{EC} \pm \nu_{LFO}$ originating from the mixing of external-cavity frequency ν_{EC} and LFO frequency ν_{LFO}, which is the indication of regular PPO are not observed. The broad peaks for ν_{EC} and ν_{LFO} mean that the intensity noise is increased strongly, and the dynamics of the laser system is more complex. When the operating current is increased to 250 mA, the time series in **Figure 12(b)** shows irregular PPO, and the high-frequency external-cavity oscillation is not as clear as in the condition of low injected current. The average duration of the pulse package is less than 20 ns. The broad peaks for ν_{EC} and ν_{LFO} mean the dynamic behavior of the laser system is more complex. The pulse package is not clear with the operated current of 340 mA, and the pulses

occurring at the external-cavity delay interval are almost invisible, as shown in **Figure 12(c)**. Finally, the time series shows a chaotic behavior with an injected current of 420 mA. The corresponding intensity noise spectra for the injected currents of 340 and 420 mA are shown in **Figure 12(g, h)**. The peak for LFO is not observed, and the broad intensity noise spectra from low to high frequency indicate typical chaotic dynamics of the output beam.

The external-cavity feedback is classified into two regimes: short- and long-cavity regimes. When the relaxation oscillation frequency of the solitary diode laser, ν_{RO}, is lower than ν_{EC}, the feedback is in short-cavity regime; otherwise, it is in long-cavity regime [26, 38, 39]. Regular PPO was first observed in 2001 by Heil et al. in short-cavity feedback narrow-strip diode laser systems [26]. With moderate feedback strength, the previous study shows that the PPO mainly takes place in the diode laser with short-cavity feedback, while LFF and chaos take place in the long-cavity regime [29, 38]. Recently, we observed regular PPO in a BAL with a lateral-mode-selected long-cavity feedback [36]. Here, regular PPO is observed in a BAL with grating external-cavity feedback. Different routes to chaos in different ECDL systems have been found [23, 40], here, we observe the transition from regular PPO to chaos in the green GaN BAL with grating external-cavity feedback.

Normally, an external-cavity length of a few centimeters is classified into short-cavity regime, thus in this point, the 33 cm external-cavity length in our case is in the long-cavity regime. The ν_{RO} of the solitary diode laser is proportional to the square root of the difference between the injected current and the solitary laser threshold current [38, 39]. This means the definition of ν_{RO} is valid only when the injected current is higher than the threshold current of the solitary laser, and the classification of short- and long-cavity regime is meaningful only on such condition. In our experiment, the PPO mainly takes place with the operating current lower than the threshold of the solitary laser. In this point, this is a new regime for the ECDL system.

In summary, the dynamics of the green high-power ECDL system with grating feedback operated in *p*-polarized mode is investigated. As the increase of the injected current, different dynamic behaviors from regular PPO, irregular PPO, to chaos are observed.

4. Conclusion

Both blue and green high-power, tunable, narrow-bandwidth ECDL systems based on GaN broad-area diode lasers and external grating feedback are demonstrated. For the blue ECDL, two gratings are applied. The holographic grating is for obtaining high power, a 530 mW output power with a tunable range of 1.4 nm is obtained with this grating; the ruled grating is for achieving broad tunable range, an output power of 80 mW with a tunable range of 6.0 nm is achieved with the ruled grating. For the green ECDL, the laser system can be operated in two modes, for *p*-polarized mode operation, an output power of 50 mW with a tunable range of 9.2 nm is obtained; for *s*-polarized mode operation, an output power of 480 mW with a tunable range of 2.1 nm is achieved.

The tuning range and the output power optimization of an external-cavity diode laser system with grating feedback is investigated based on the experimental results on the blue and green

ECDL systems and diode laser theory. The obtained results can be used as a guide to select grating for an ECDL system for different applications. The dynamic behavior of the green ECDL system operated in *p*-polarized mode is studied. As the increase of the injected current, different dynamic states, such as regular PPO, irregular PPO and chaos are observed.

Acknowledgements

This work was supported in part by the Danish Energy Technology Development and Demonstration Program (EUDP) under Grant 64014-0171.

Author details

Mingjun Chi*, Ole Bjarlin Jensen, Anders Kragh Hansen and Paul Michael Petersen

*Address all correspondence to: mchi@fotonik.dtu.dk

DTU Fotonk, Department of Photonics Engineering, Technical University of Denmark, Roskilde, Denmark

References

[1] Nakamura S, Senoh M, Nagahama S, Iwasa N, Yamada T, Matsushita T, Sugimoto Y, Kiyoku H. Room-temperature continuous-wave operation of InGaN multi-quantum-well structure laser diodes. Applied Physics Letters. 1996;**69**:4056-4058. DOI: 10.1063/1.117816

[2] http://www.nichia.co.jp

[3] Kang JH, Wenzel H, Hoffmann V, Freier E, Sulmoni L, Unger RS, Einfeldt S, Wernicke T, Kneissl M. DFB laser diodes based on GaN using 10^{th} order laterally coupled surface gratings. IEEE Photonics Technology Letters. 2018;**30**:231-234. DOI: 10.1109/LPT.2017.2780446

[4] Holc K, Bielecki Z, Wojtas J, Perlin P, Goss J, Czyzewski A, Magryta P, Stacewicz T. Blue laser diodes for trace matter detection. Optica Applicata. 2010;**40**:641-651

[5] Tanaka T, Takahashi K, Sako K, Kasegawa R, Toishi M, Watanabe K, Samuels D, Takeya M. Littrow-type external-cavity blue laser for holographic data storage. Applied Optics. 2007;**46**:3583-3592. DOI: 10.1364/AO.46.003583

[6] Shimada Y, Chida Y, Ohtsubo N, Aoki T, Takeuchi M, Kuga T, Torii Y. A simplified 461-nm laser system using blue diodes and a hollow cathode lamp for laser cooling of Sr. The Review of Scientific Instruments. 2013;**48**:063101. DOI: 10.1063/1.4808246

[7] Hofmann J, Blume G, Jedrzejczyk D, Eppich B, Feise D, Kreutzmann S, Sahm A, Paschke K. Miniaturized diode laser module emitting green light at 532 nm with a power of more

than 900 mW for next-generation holographic displays. Optical Review. 2016;**23**:141-145. DOI: 10.1007/s10043

[8] Müller A, Marschall S, Jensen OB, Fricke J, Wenzel H, Sumpf B, Andersen PE. Diode laser based light sources for biomedical applications. Laser & Photonics Reviews. 2013;**7**:605-627. DOI: 10.1002/lpor.201200051

[9] Ruhnke N, Müller A, Eppich B, Maiwald M, Sumpf B, Erbert G, Tränkle G. Compact deep UV system at 222.5 nm based on frequency doubling of GaN laser diode emission. IEEE Photonics Technology Letters. 2018;**30**:289-292. DOI: 10.1109/LPT.2017.2787463

[10] Gürel K, Wittwer VJ, Hoffmann M, Saraceno CJ, Hakobyan S, Resan B, Rohrbacher A, Weingarten K, Schilt S, Südmeyer T. Green-diode-pumped femtosecond Ti: Sapphire laser with up to 450 mW average power. Optics Express. 2015;**23**:30043-30048. DOI: 10.1364/OE.23.030043

[11] Fiebig C, Sahm A, Uebernickel M, Blume G, Eppich B, Paschke K, Erbert G. Compact second-harmonic generation laser module with 1 W optical output power at 490 nm. Optics Express. 2009;**17**:22785-22790. DOI: 10.1364/OE.17.022785

[12] Hansen AK, Andersen PE, Jensen OB, Sumpf B, Erbert G, Petersen PM. Highly efficient single-pass sum frequency generation by cascaded nonlinear crystals. Optics Letters. 2015;**40**:5526-5529. DOI: 10.1364/OL.40.005526

[13] Ruhnke N, Müller A, Eppich B, Maiwald M, Sumpf B, Erbert G, Tränkle G. 400 mW external cavity diode laser with narrowband emission at 445 nm. Optics Letters. 2014;**39**:3794-3797. DOI: 10.1364/OL.39.003794

[14] Chen YH, Lin WC, Chen HZ, Shy JT, Chui HC. Single-frequency external cavity green diode laser. IEEE Photonics Journal. 2017;**9**:1507207. DOI: 10.1109/JPHOT.2017.2776284

[15] Chi M, Jensen OB, Petersen PM. Tuning range and output power optimization of an external-cavity GaN diode laser at 455 nm. Applied Optics. 2016;**55**:2263-2269. DOI: 10.1364/AO.55.002263

[16] Chi M, Jensen OB, Petersen PM. Green high-power tunable external-cavity GaN diode laser at 515 nm. Optics Letters. 2016;**41**:4154-4157. DOI: 10.1364/OL.41.004154

[17] Unger P. Introduction to power diode lasers. In: Diehl R, editor. High-Power Diode Lasers, Fundamentals, Technology, Applications. Berlin Heidelberg: Springer-Verlag; 2000. pp. 37-46

[18] Conroy RS, Hewett JJ, Lancaster GPT, Sibbett W, Allen JW, Dholakia K. Characterisation of an extended cavity violet diode laser. Optics Communication. 2000;**175**:185-188. DOI: 10.1016/S0030-4018(99)00742-7

[19] Lonsdale DJ, Willis AP, King TA. Extended tuning and single-mode operation of an anti-reflection-coated InGaN violet laser diode in a Littrow cavity. Measurement Science and Technology. 2002;**13**:488-493. DOI: 10.1088/0957-0233/13/4/310

[20] Soriano MC, García-Ojalvo J, Mirasso CR, Fischer I. Complex photonics: Dynamics and applications of delay-coupled semiconductors lasers. Reviews of Modern Physics. 2013;**85**:421-470. DOI: 10.1103/RevModPhys.85.421

[21] Sciamanna M, Shore KA. Physics and applications of laser diode chaos. Nature Photonics. 2015;**9**:151-162. DOI: 10.1038/nphoton.2014.326

[22] Chi M, Jensen OB, Hansen AK, Petersen PM. Dynamics of a green high-power tunable external-cavity broad-area GaN diode laser. Journal of the Optical Society of America B: Optical Physics. 2018;**35**:667-671. DOI: 10.1364/JOSAB.35.000667

[23] Ye J, Li H, McInerney JG. Period-doubling route to chaos in a semiconductor laser with weak optical feedback. Physical Review A. 1993;**47**:2249-2252. DOI: 10.1103/PhysRevA.47.2249

[24] Hohl A, Gavrielides A. Bifurcation cascade in a semiconductor laser subject to optical feedback. Physical Review Letters. 1999;**82**:1148-1151. DOI: 10.1103/PhysRevLett.82.1148

[25] Lawrence JS, Kane DM. Contrasting conventional optical and phase-conjugate feedback in laser diodes. Physical Review A. 2001;**63**:033805. DOI: 10.1103/PhysRevA.63.033805

[26] Heil T, Fischer I, Elsäβer W, Gavrielides A. Dynamics of semiconductor lasers subject to delayed optical feedback: The short cavity regime. Physical Review Letters. 2001; **87**:243901. DOI: 10.1103/PhysRevLett.87.243901

[27] Mandre SK, Fischer I, Elsässer W. Control of the spatiotemporal emission of a broad-area semiconductor laser by spatially filtered feedback. Optics Letters. 2003;**28**:1135-1137. DOI: 10.1364/OL.28.001135

[28] Mandre SK, Fischer I, Elsässer W. Spatiotemporal emission dynamics of a broad-area semiconductor laser in an external cavity: Stabilization and feedback-induced instabilities. Optics Communication. 2005;**244**:355-365. DOI: 10.1016/j.optcom.2004.09.058

[29] Takeda A, Shogenji R, Ohtsubo J. Dynamics and pulse-package oscillations in broad-area semiconductor lasers with short optical feedback. Applied Physics Letters. 2012; **101**:231105. DOI: 10.1063/1.4769181

[30] Lawrence JS, Kane DM. Broad-area diode lasers with plane-mirror and phase-conjugate feedback. Journal of Lightwave Technology. 2002;**20**:100-104. DOI: 10.1109/50.974824

[31] Fujita Y, Ohtsubo J. Optical-feedback-induced stability and instability in broad-area semiconductor lasers. Applied Physics Letters. 2005;**87**:031112. DOI: 10.1063/1.1999850

[32] Arahata M, Uchida A. Inphase and antiphase dynamics of spatially-resolved light intensities emitted by a chaotic broad-area semiconductor laser. IEEE Journal of Selected Topics in Quantum Electronics. 2015;**21**:1800609. DOI: 10.1109/JSTQE.2015.2422473

[33] Vasil'ev PP, White IH. Phase-conjugation broad area twin-contact semiconductor laser. Applied Physics Letters. 1997;**71**:40-42. DOI: 10.1063/1.119462

[34] Tachikawa T, Shogenji R, Ohtsubo J. Observation of multi-path interference in broad-area semiconductor lasers with optical feedback. Optical Review. 2009;**16**:533-539. DOI: 10.1007/s10043-009-0105-5

[35] Wolff S, Rodionov A, Sherstobitov VE, Doering C, Fouckhardt H. Self-pulsation in broad-area lasers with transverse-mode selective feedback. Optics Communication. 2006; **265**:642-648. DOI: 10.1016/j.optcom.2006.04.008

[36] Chi M, Petersen PM. Dynamics of a broad-area diode laser with lateral-mode-selected long-cavity feedback. Journal of Applied Physics. 2014;**116**:103101. DOI: 10.1063/1.4894628

[37] Pan M, Evans DJ, Gray GR, Smith LM, Benner RE, Johnson CW, Knowlton DD. Spatial and temporal coherence of broad-area lasers with grating feedback. Journal of the Optical Society of America B: Optical Physics. 1998;**15**:2531-2536. DOI: 10.1364/JOSAB.15.002531

[38] Toomey JP, Kane DM, McMahon C, Argyris A, Syvridis D. Integrated semiconductor laser with optical feedback: Transition from short to long cavity regime. Optics Express. 2015;**23**:18754-18762. DOI: 10.1364/OE.23.018754

[39] Heil T, Fischer I, Elsäβer W, Krauskopf B, Green K, Gavrielides A. Delay dynamics of semiconductor lasers with short external cavities: Bifurcation scenarios and mechanisms. Physical Review E. 2003;**67**:066214. DOI: 10.1103/PhysRevE.67.066214

[40] Li N, Susanto H, Cemlyn BR, Henning ID, Adams MJ. Stability and bifurcation analysis of spin-polarized vertical-cavity surface-emitting lasers. Physical Review A. 2017; **96**:013840. DOI: 10.1103/PhysRevA.96.013840